Catalysis Letters
https://doi.org/10.1007/s10562-020-03135-w

Synthesis of Ionic Liquids as Novel Nanocatalysts for Fixation of Carbon Dioxide with Epoxides by Using a Carbon Dioxide Balloon

Pu Zhang[1] · **Rahele Zhiani**[2,3]

Received: 16 December 2019 / Accepted: 1 February 2020
© Springer Science+Business Media, LLC, part of Springer Nature 2020

Abstract

In the present study, the nanocatalyst of imidazolium based ionic liquids (ILs) is synthesized for the fixation of carbon dioxide (CO_2) under moderate conditions by utilizing a balloon of CO_2 with commercially available epoxides. IL incorporated porous dendritic fibrous nanosilica (DFNS) catalyst (IL/DFNS) was designed and synthesized. The synthesized catalyst was characterized using N_2 absorption desorption isotherm, XPS, SEM, EDX, TGA, HR-TEM, and AFM. For cyclic carbonate, an environmental friendly catalyst of porous IL/DFNS indicate highly impressive catalytic efficiency from CO_2 through CO_2 fixation and epoxides under mild condition. Attendance of polar hydroxyl and anion exchange nature groups of IL frame work to high surface area is known as the main aspect to be reliable for elevated catalytic efficiency and also advance in stability of catalyst and providing a proper recyclability.

Graphic Abstract

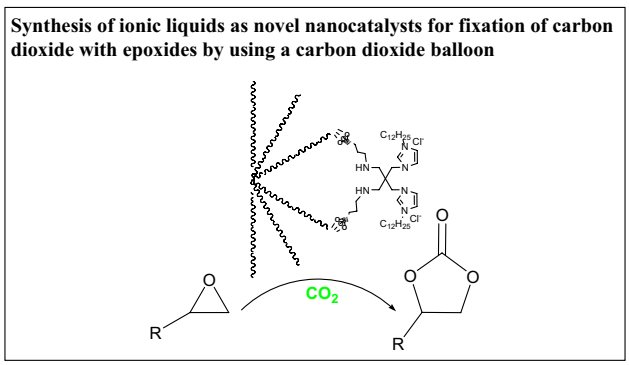

Keywords Nano catalyst · One-pot synthesis · Green chemistry · Carbon dioxide

1 Introduction

Because of environmental convenience and sustainable increasing from the usage of renewable sources and the rising concentration of emissions, the CO_2 exploitation, as a green source of carbon for the manufacture of valuable added chemical intermediates is garnered higher attention in the recent studies [1–5]. Consequently, taking necessary steps to control the emission of the industrial raw materials by flue-gas capture and converting it to favorable economically competitive products are important tasks [2, 6–13]. In this regards, scholars across the globe are

✉ Pu Zhang
puzhanglvliang@sina.com

✉ Rahele Zhiani
r_zhiani2006@yahoo.com

[1] Department of Chemistry and Chemical Engineering, Lvliang University, lvliang 033000, Shanxi, China

[2] New Materials Technology and Processing Research Center, Department of Chemistry, Neyshabur Branch, Islamic Azad University, Neyshabur, Iran

[3] Young Researchers and Elite Club, Neyshabur Branch, Islamic Azad University, Neyshabur, Iran

Published online: 12 February 2020

currently concerning for invention of novel protocols that may properly capture the atmospheric CO_2 and then convert it to value-added substances [14–17]. However, there are different challenges in the case of developing green and highly efficient ways for CO_2 fixation reaction under green conditions [18–21].

The organocatalysis presents an alternative for the CO_2 fixation and activation utilizing small organic molecules that is known as catalysts. Recently, [22–29] *N*-heterocyclic carbenes (NHCs) [30–32], frustrated Lewis pairs (FLPs) [33–39], *N*-heterocyclic bases (NHCBs), [40–43] polyphenols, [44, 45] quaternary onium hydroxide/quaternary [46] onium salts (PTCs), and fluoroalcohols, silanediols with co-catalysts [47, 48] as well as ionic liquids (ILs) [49–53] are utilized as catalysts for catalytic CO_2 fixation and activation.

In recent years, the use of surfactant on soft templating is an efficient way to produce mesoporous silica (dendrimetic silica fibers morphology (DFNS)). For adsorption and catalysis approaches as support material, silica having this morphology are being examined. In order to access the functional materials more effectively, for reactants, the outward radial widening of these silicas has higher surface area. Moreover, DFNS possesses thermally stable, and intrinsic mesoporous properties and presents high activity. The DFNS is required to synthesis micro emulsion system, which has surfactant, water, and oil. Moreover, the particle size and DFNS morphology may be lightly manipulated utilizing co-surfactant and different co solvents [54–57].

Ionic liquids (ILs) is introduced as proper homogeneous catalysts [58] due to their outstanding physicochemical properties such as negligible wide liquid range, vapour pressure, excellent solubility, and high ionic conductivity [59]. Although ILs have many advantages but, in its recovery, their practical usages are restricted utilizing some difficulties that cause environmental and economic issues (i.e., pending catalytic reactions, their high viscosity not just limits their mass transfer but also causes their handling hard). In addition, the utilize of relatively large values of ILs can cause toxicological issues and is costly. To produce heterogeneous catalysts, these issues may be overcome by utilizing immobilization of ILs on solid supports [60–62].

The aim of this study is production of new imidazolium based ILs to be utilized as nanocatalyst in the CO_2 fixation with epoxides in order to provide cyclic carbonates in good to excellent yields in very moderate conditions. Imidazolium based ionic liquids are produced. To give IL, the synthesis approach is according to attach dodecyl bromide to imidazole ring to obtain dodecyl imidazole and pairing two dodecyl imidazoles by utilizing 1,3-Diamino-2,2-bis(bromomethyl)propane, subsequently. This IL attaching by etherification on DFNS nanoparticle surfaces (Scheme 1).

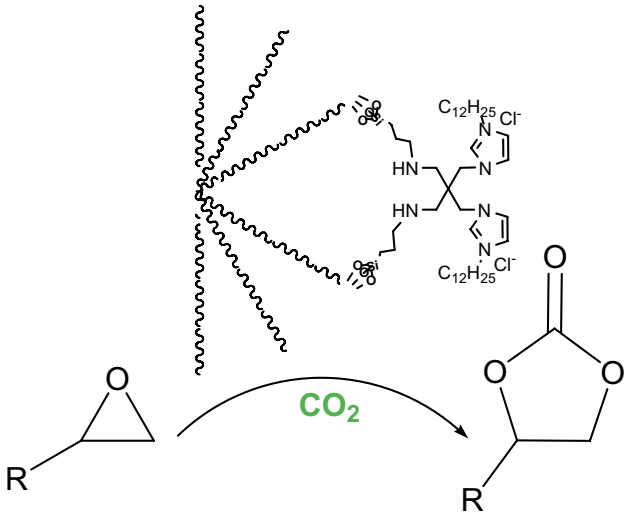

Scheme 1 Bifunctional phase-transfer catalysts for CO_2 fixation

2 Experimental

2.1 General Procedure for the Preparation of IL

6 mmol of imidazole, 6 mmol of potassium hydroxide and 2 ml of dimethylesulfoxide were introduced into a 10 ml flask and were mixed by stirrer at room temperature for 2 h. Then, 5 mmol of dodecylboromide were added drop wise to the reaction mixture in 30 min. The mixture was stirred for another 4 h. Afterwards, 30 ml of water was added to the reaction mixture and then the flask contents were introduced into a separating funnel. The mixture was extracted with 30 ml batches of chloroform for five times. Then, the chloroform extracts were combined and washed with 30 ml batches of water for five times to remove unreacted imidazole. The chloroform extract was dried with excess of $MgSO_4$. 1mmole of 2,2,-bis (bromomethyl) propane-1,3-diamine and 2.5 mmol of dodecyl imidazole were weighed and introduced into a 25 mL flask and subsequently the mixture was placed in a 150 °C oil bath. After 8 h, the reaction a dark brown gelatinous substance was obtained. For purification, the product was washed two times with acetone and three times with acetonitrile.

2.2 General Procedure for the Preparation of FPS

Tetraethyl orthosilicate (2.08 g) and tripolyphosphate (3.67 g) were dissolved in a solution of cyclohexane (30 mL) and 1-pentanol (1.5 mL). A stirred solution of CPB (1 g) and urea (0.5 g) in water (30 mL) was then added to the top mixture. The resulting mixture was

continually stirred for 45 min at room temperature and then placed in a teflon-sealed hydrothermal reactor and heated at 120 °C for 5 h. The FPS was then isolated by centrifugation, washed with deionized water and acetone, and dried in a drying oven.

2.3 Total Approach for the Synthesis of DFNS/3-Chloromopropyl MNPs

A mixture was prepared by mixing 200 mg of $FeNi_3$/DFNS in 20 ml of THF followed by the addition of 20 mmol of NaH via ultrasonication. After that, 22 mmol of 3-chloromopropyl trimethoxysilane were added into the mixture at room temperature and stirred for 16 h at 50 °C. The resultant mixture was filtered and washed with ethanol and deionized water. The filtered solids were then dried in vacuum condition at 50 °C for 3 h.

2.4 Total Approach for the Synthesis of IL/DFNS NPs

DFNS/3-chloromopropyl (200 mg) are diffused in a solution (80 mL) of ethanol, deioned water (20 mL) and 28 wt% concentrated ammonia aqueous solution ($NH_3{\cdot}H_2O$, 2.0 mL) and finally by adding 20 mg of IL. The produced suspension has been washed, repeatedly, after intense stirring filtered frequently and then dried under the temperature of 50 °C at air presence.

2.5 General Procedures for Preparation of Cyclic Carbonate

IL/DFNS NPs (5 mg) and epoxide derivatives (1 mmol) were charged into the reactor vessel without using any co-solvent. The reactor vessel was placed under a constant pressure of carbon dioxide and then heated to 70 °C for 2 h. Then the reactor was cooled to ambient temperature, and the resulting mixture was transferred to a 50 mL round bottom flask. Upon completion, the progress of the reaction was monitored by TLC when the reaction was completed, EtOH was added to the reaction mixture and the KCC-1/IL/HPW NPs was separated by filteration. Then the solvent was removed from solution under reduced pressure and the resulting product purified by recrystallization using n-hexane/ethyl acetate.

3 Results and Discussion

In this study, solution of DFNS is synthesized with taking into account of reported approaches and after that became suitable utilizing (3-Cloropropyl)trimethoxysilane, followed by reductive amination for making the related co-immobilized IL. Scheme 2 shows this process.

The morphology of the produced nanoparticles of DFNS and IL/DFNS were evaluated by TEM and FE-SEM. Figure 1a demonstrated that there are silica fibers and layer of nonporous silica. Figure 1a and b shows TEM and FE-SEM images. As can be observed, the DFNS samples possess a wrinkled radial structure and additionally solid spheres with 400 nm diameter. Wrinkled fibers (7 nm) can be observed by close study of these images. These fibers commonly grown from the center of spheres and radially adjusted. Moreover, the wrinkled radial structure overlap makes the conical pores and this hierarchical open channel structure along with fibers may lead to transfer the mass of reactants for performing easier. In addition, it can rise access to active sites. As can be seen in Fig. 1b and d,

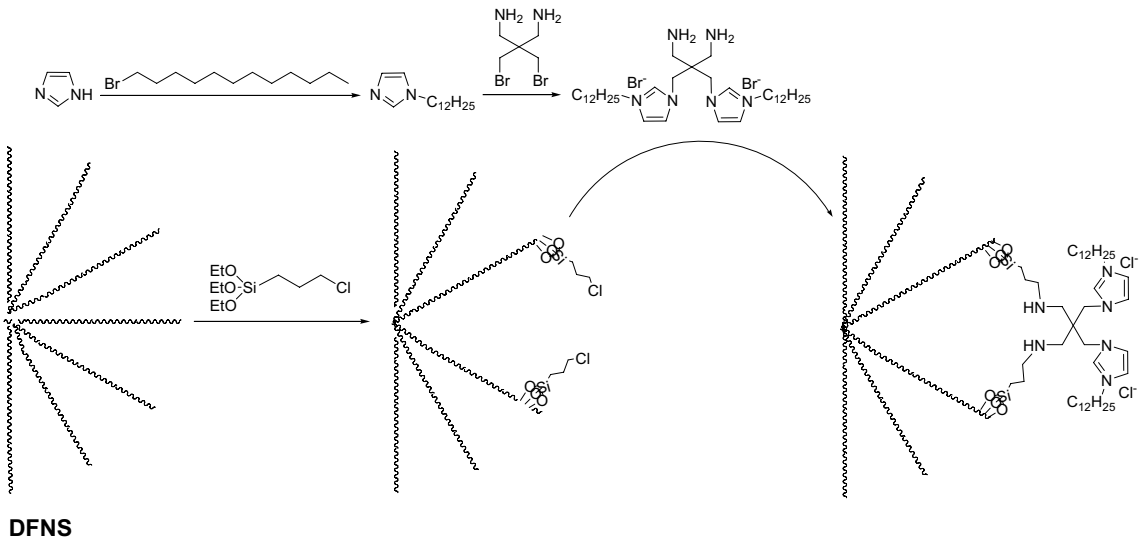

Scheme 2 Schematic illustration of the IL/DFNS NPs preparation

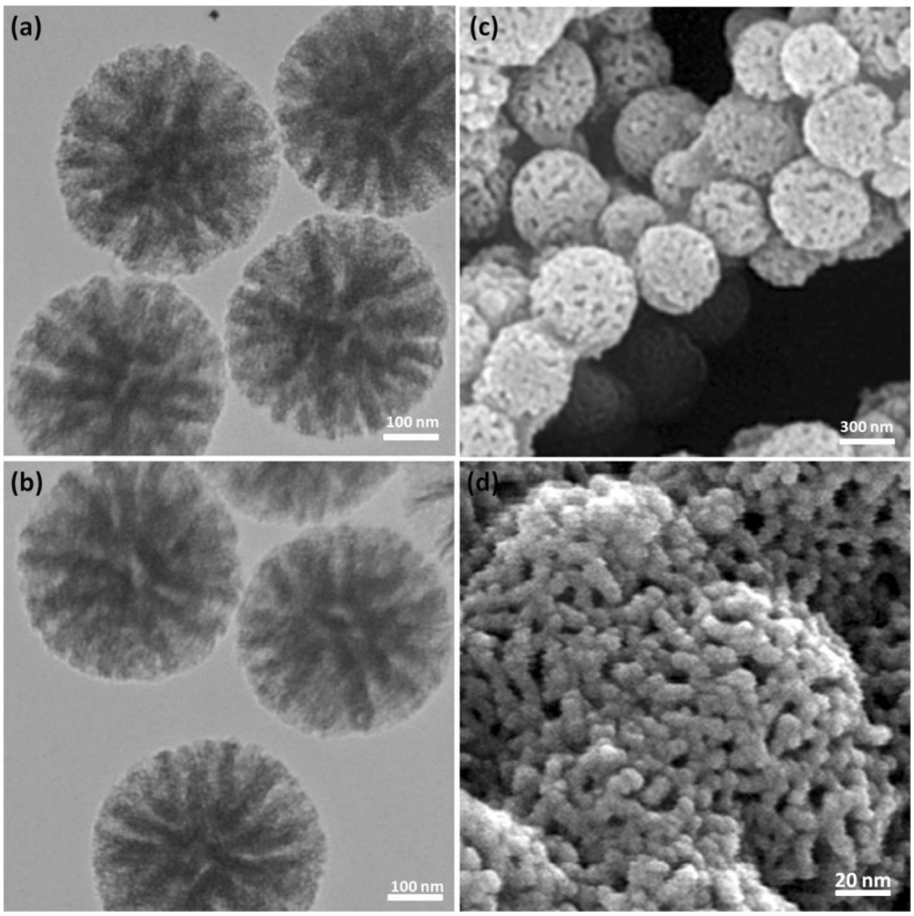

Fig. 1 TEM images of DFNS MNPs (**a**); IL/DFNS NPs (**b**); FE-SEM images of DFNS NPs (**c**); IL/DFNS NPs (**d**)

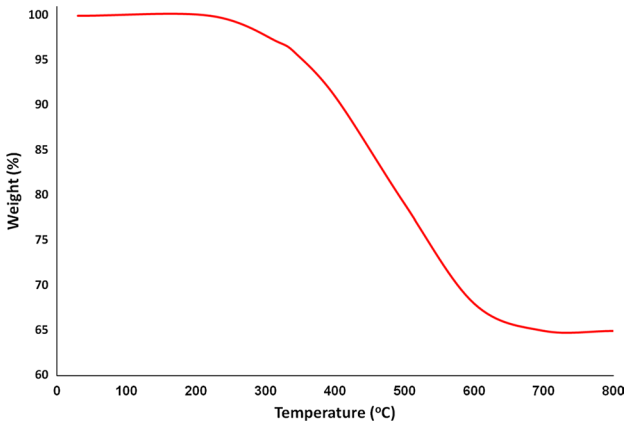

Fig. 2 TGA curves of IL/DFNS NPs

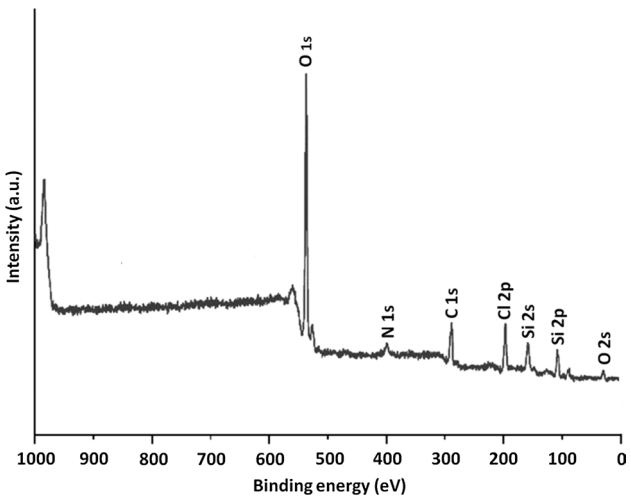

Fig. 3 XPS spectra of IL/DFNS NPs

after modification, the morphology of DFNS did not vary from FE-SEM and TEM images of IL/DFNS NPs. TGA analysis of IL/DFNS NPs is proved in Fig. 2. The solvent deletion of physisorbed and chemisorbed on the IL/DFNS material surface causing the weight loss. Moreover, the weight loss in the temperature between 250–450 °C is near 28.1 wt%, which is related to the organic group derivatives. Factually, due to exiting the DFNS NPs, the residual mass after the decomposition of nanoparticles of IL/DFNS.

In this work, we use XPS for studying the chemical sections on the IL/DFNS NPs level. For the as gathered catalyst,

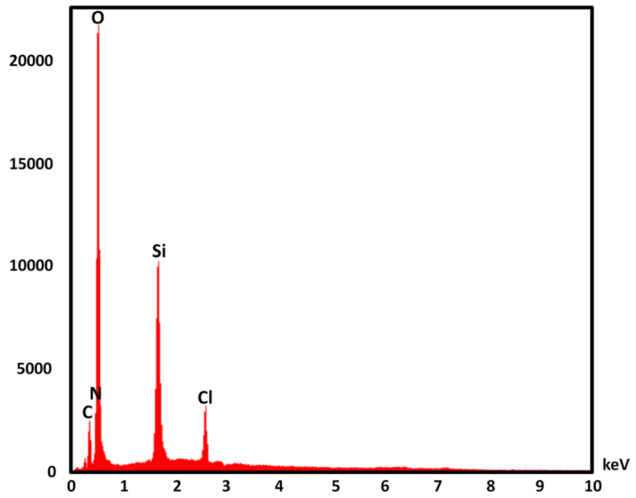

Fig. 4 EDX spectra of IL/DFNS NPs

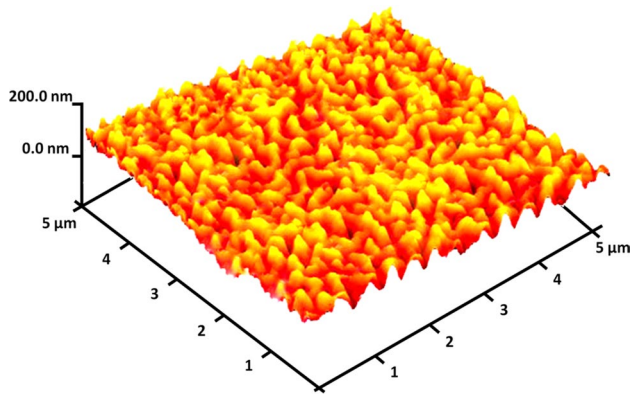

Fig. 5 Three-dimensional of AFM images of IL/DFNS NPs

Table 1 Structural parameters of DFNS, and the IL/DFNS NPs

Catalysts	S_{BET} ($m^2\ g^{-1}$)	V_a ($cm^3\ g^{-1}$)	D_{BJH} (nm)
DFNS	671	3.2	9
IL/DFNS	348	1.4	5

Table 2 Synthesis of cyclic carbonate by IL/DFNS NPs in different solvents

Entry	Solvent	Time (h)	Yield (%)[a]
1	H_2O	4	–
2	MeOH	4	–
3	EtOH	4	–
4	*i*-PrOH	4	–
5	Dioxane	4	–
6	*n*-Hexane	4	–
7	$CHCl_3$	4	31
8	CH_2Cl_2	4	33
9	DMF	4	19
10	THF	4	28
11	DMSO	4	27
12	CH_3CN	4	22
13	EtOAc	4	38
14	Toluene	4	48
15	Anisole	4	49
16	Solvent-free	4	98
17	Solvent-free	3	98
18	Solvent-free	2	98
19	Solvent-free	1	71

Reaction conditions: propylene oxide (1 mmol), IL/DFNS NPs (10 mg), and CO_2 1.5 MPa, at 120 °C

[a]Isolated yields

Fig. 3 demonstrates a scheme of XPS. Peaks of C, O, Cl, and N are shown and the existence of N1s additional confirmed that DFNS are functionalized using the imidazolium. Moreover, the attendance of ions of Cl^- (the imidazolium counter ion) was specified by a sharp peak (in 287 eV). This demonstrates that there is imidazolium moiety into the catalyst. Figure 4 shows the origins in the catalyst that determined by EDX analysis. Figure 4 indicates the pattern of EDX showed whole the elements, which stand in IL/DFNS NPs like nitrogen, silicon, carbon, oxygen, and chlorine. These NPs level roughness is specified by AFM (atomic force microscopy) analysis. Figure 5 shows topographic scheme and the more height region demonstrated by the brighter yellowish white color enhanced by decreasing T/W, suggesting the increased in the level roughness of catalyst.

N_2 adsorption–desorption isotherm analysis is done to analyze the specific surface area and porosity of the products. In accordance to the BJH method, the mean pore diameter and the specific surface area as well as the total pore volume values are shown in Table 1. The BET results demonstrated that the active surface area of the IL/DFNS and DFNS are equal to 348 and 671 $m^2\ g^{-1}$, respectively. The results of our experiments showed that the specific surface area decreased after melamine intercalation. In addition, the pore volume and average pore radius increased using melamine. It was determined that melamine intercalation has a more porous network structure.

In this apparatus, the conditions of reaction are optimized by propylene oxide and carbon dioxide for the production of cyclic carbonates catalyzed by nanoparticles of IL/DFNS. The influences of various parameters like time and solvent on the model reaction are presented in Table 2. Various solvents are utilized to study their effect on the synthesis of cyclic carbonates. Our outcomes indicated that no product is produced by polar protic solvents like isopropanol, methanol, ethanol, and water. Polar protic solvents like

EtOAc, DMF, and DMSO demonstrated that moderate performance in cross-coupling yields. In the present study, the outcomes indicated that solvents are less efficient compared to common heating under solvent-free conditions. The cross-coupling reaction efficiency in the case of carbonylation is higher in less polar solvents like toluene and/or anisole. The reaction is done under optimum conditions in the attendance of IL/DFNS NPs (10 mg) and the progress of reaction is analyzed by utilizing GC to study the reaction time. We found that proper product yields are archived after 120 min.

The influences of various factors for the model reaction are studied by IL/DFNS nanoparticles. As can be observed in Fig. 6, like other factors, the catalyst value is impressive in yields. In addition, low the product yields of the cycloaddition reaction are achieved in the lack of the catalyst. The cyclic carbonate products demonstrated moderate yields using weighted quantities of IL/DFNS NPs (1–4 mg). The optimum value of IL/DFNS NPs for the model reaction is determined to be 5 mg.

The effect of temperature on the reaction is shown in Fig. 7. As observed, cyclic carbonate production enhanced to around 98% at the temperature of 70 °C under 1.0 MPa CO_2 pressure after 120 min. Nevertheless, because of a negligible value of specific by products like olefin isomerization, a further enhance in temperature caused in a slight reduce in the amount of the product. Thus, for the parallel reactions of CO_2 and epoxide, the optimum temperature is around 70 °C. The pressure of CO_2 had a considerable influence on the parallel reaction. As observed in Fig. 8, the rate of reaction enhanced under pressures in the range of 0.8 and 1.0 Mpa, rapidly. Based on previous works, we have concluded that enhancing the reaction pressure is desirable for cyclic carbonate synthesis until the pressure is below 1.0 MPa. Thus, the CO_2 pressure of 1.0 MPa is recognized as a particular condition. Initially, the following conditions are considered for the reaction: (the temperature of 70 °C at 4 h (10 mol%)). Various oxidants are utilized for enhancing yields of product. The reaction product is highly sensitive to the base.

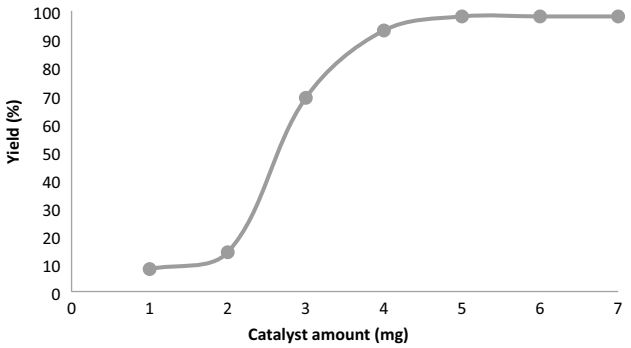

Fig. 6 Effect of increasing amount IL/DFNS NPs on yield of cyclic carbonate

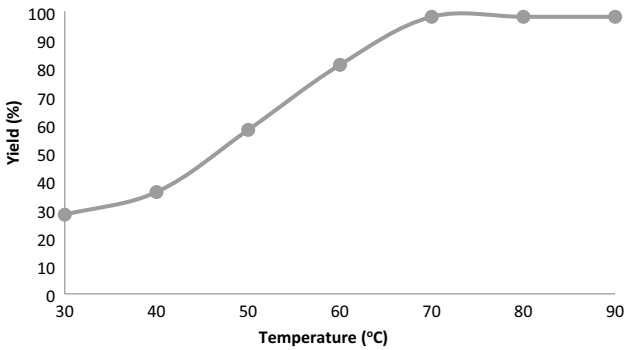

Fig. 7 Effect of temperature on yield of cyclic carbonate

As seen in Table 3, various epoxides are studied in the case of the investigation of the substrate scopes in this novel one-pot approach for the production of cyclic carbonates. Table 3 shows that, for all substrate, the catalyst is active. It is determined that glycidyl ethers (entry 4–12) are converted to their relating cyclic carbonates in high to excellent products, nevertheless, styrene oxides (entry 13–18) prepared carbonates in moderate products. The corresponding cyclic carbonates 2j as well as 2 k are achieved in good yields and moderate enantioselectivities while enantiopure styrene oxides 19 and 20 are utilized as substrates (78.3% and 66.7%), and the stereochemistry inversion of the cyclic carbonates may be due to the electron-withdrawing nature of the benzene ring that causes a nucleophilic ring opening of styrene oxide at the methylene bond and the methine bond.

We compared the catalytic performance of our catalyst with literature reported catalysts for the synthesis of cyclic carbonate. Table 4 clearly demonstrates that lower temperature, the minimum amount of catalyst, lower pressure of carbon dioxide and shorter reaction time were required for CO_2 transformation, using IL/DFNS NPs, while an appropriate, highly perfect, performance of the present catalyst was observed for the this reaction.

The mechanism of the bifunctional phase-transfer IL/DFNS NPs according to the experimental facts in the case

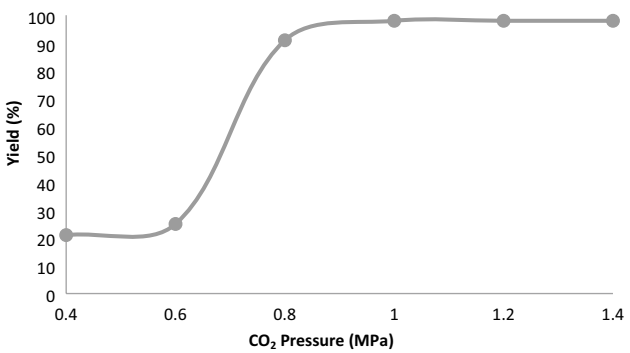

Fig. 8 Effect of CO_2 pressure on the synthesis of cyclic carbonate

Table 3 Synthesis of cyclic carbonate derivatives catalyzed by IL/DFNS NPs

Entry	Epoxides	Product	Yield (%)[b]
1	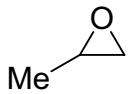	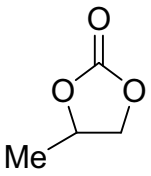	98
2	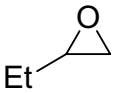	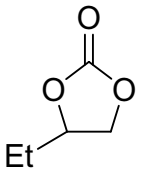	91
3	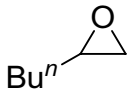	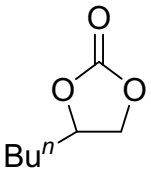	92
4	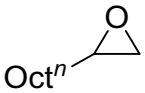	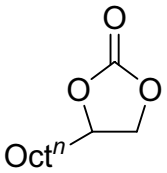	86
5	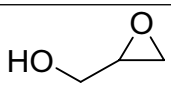	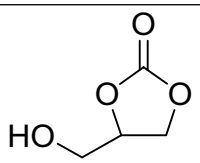	94
6	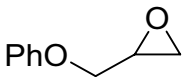	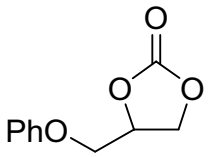	98
7	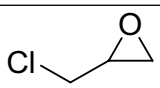	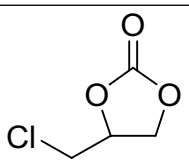	96
8	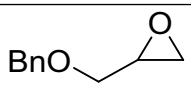	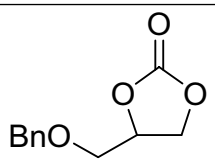	98

Table 3 (continued)

9	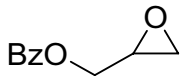	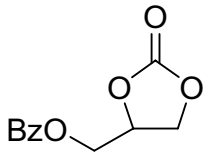	95
10	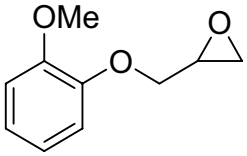	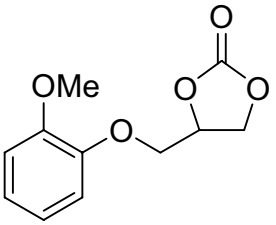	96
11	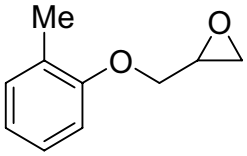	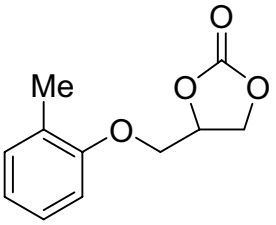	93
12	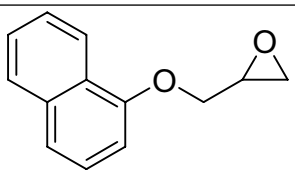	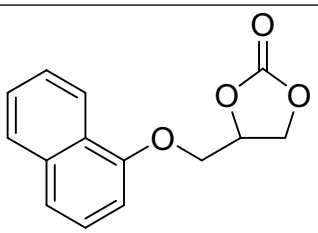	82
13	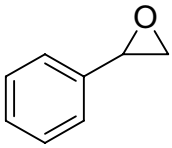	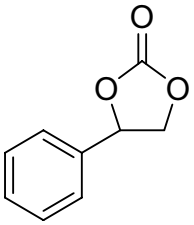	78
14	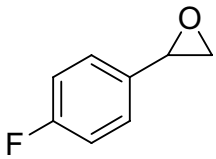	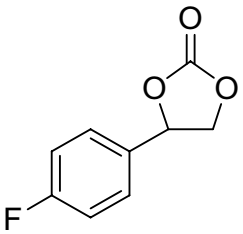	75
15	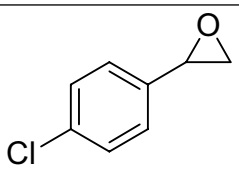	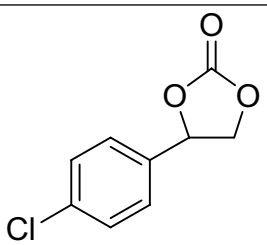	79

Table 3 (continued)

16	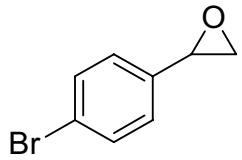	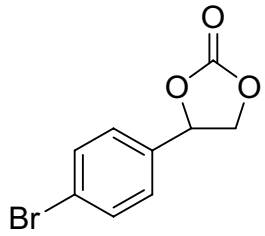	77
17	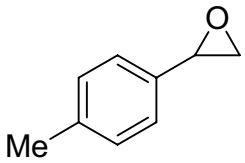	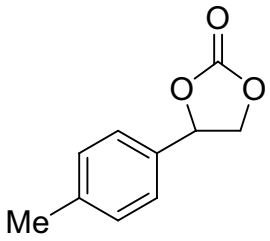	83
18	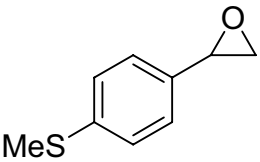	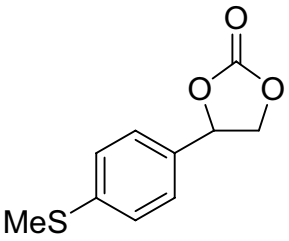	85
19	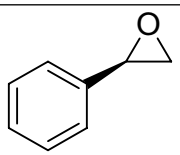	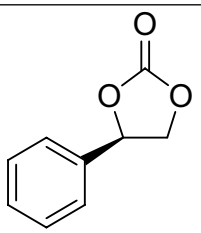	80 78 *ee*
20	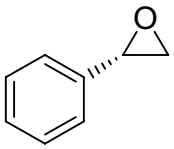	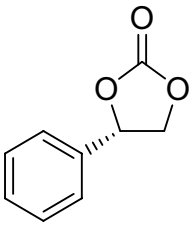	81 75 *ee*

[a]Reaction condition: epoxide derivatives (1 mmol), IL/DFNS NPs (5 mg), CO_2 1 Mpa (balloon), 2 h

[b]Yield refers to isolated product

of the fixation of carbon dioxide with epoxides was suggested in Scheme 3. Firstly, epoxide was activated using IL/DFNS via hydrogen-bonding interaction among atoms of O and N–H for forming intermediate A that endures a nucleophilic attack of Cl^- to provide intermediate B that then attacks carbon dioxide to get intermediate C, and after that the intramolecular ring-closing of intermediate C prepares cyclic carbonate with a IL/DFNS release to create the carbonate ready to the next catalytic cycle.

In the last step, we have done a leaching study to assay whether this catalytic approach is really heterogeneous or attended catalysis is increased homogeneously using some of IL materials leaching into the solution. Firstly, the reaction is conducted utilizing optimized conditions, in the attendance of a ten-runs reused batch of the catalyst. After a few minute, catalyst is taked by hot filtration and the remaining solution is stirred. Figure 9 indicates the CO_2 fixation vs time by a ten-runs reused catalyst batch (signed as a green curve),

Table 4 Comparison of the catalytic efficiency of IL/DFNS NPs with various catalysts for synthesis of cyclic carbonate

Entry	Catalyst	MPa (CO_2)	Solvent	Temperature (°C)	Amount catalyst	Time (h)	Yield (%)
1	NaBr	2	H_2O	125	1 mmol	1	30 [63]
2	KBr	2	H_2O	125	1 mmol	1	52 [63]
3	KI	2	H_2O	125	1 mmol	1	68 [63]
4	Bu_4NBr	2	H_2O	125	1 mmol	1	86 [63]
5	Bu_4NCl	2	H_2O	125	1 mmol	1	46 [63]
6	Bu_4NI	2	H_2O	125	1 mmol	1	88 [63]
7	[bmim]Br	2	H_2O	125	1 mmol	1	87 [63]
8	[bmim]Cl	2	H_2O	125	1 mmol	1	42 [63]
9	[bmim]I	2	H_2O	125	1 mmol	1	90 [63]
10	BImBr_SiO_2	3.55	–	110	1 mol (%)	6	91.7 [64]
11	GO-DMEDA-I	2	–	120	0.65 mol (%)	3	89 [65]
12	Organic–inorganic hybrid catalyst	1	–	90	1 mol (%)	6	99 [66]
13	Mim	1.5	–	120	1 mol (%)	2	– [67]
14	HBimBr	1.5	–	120	1 mol (%)	2	77.7 [67]
15	HMimBr	1.5	–	120	0.5 mol (%)	2	59.8 [67]
16	HEimBr	1.5	–	120	1 mol (%)	2	85.8 [67]
17	HMimCl	1.5	–	120	1 mol (%)	2	47.4 [67]
18	HPyBr	1.5	–	120	1 mol (%)	2	31.6 [67]
19	HTeaBr	1.5	–	120	1 mol (%)	2	34.9 [67]
20	FDU-HEIMBr	1	–	110	0.5 mol (%)	3	99 [68]
21	$Et_4N^+Cl^-$	1	–	100	1 mol (%)	24	63 [69]
22	n-$Bu_4N^+Cl^-$	1	–	100	1 mol (%)	24	61 [69]
23	n-$Bu_3MeN^+Cl^-$	1	–	100	1 mol (%)	24	58 [69]
24	IL/DFNS	1	–	70	0.5 mol (%)	2	98

Reaction conditions: epoxide (1 mmol), and CO_2 in different solvents and in different amounts of catalyst, temperature, and time

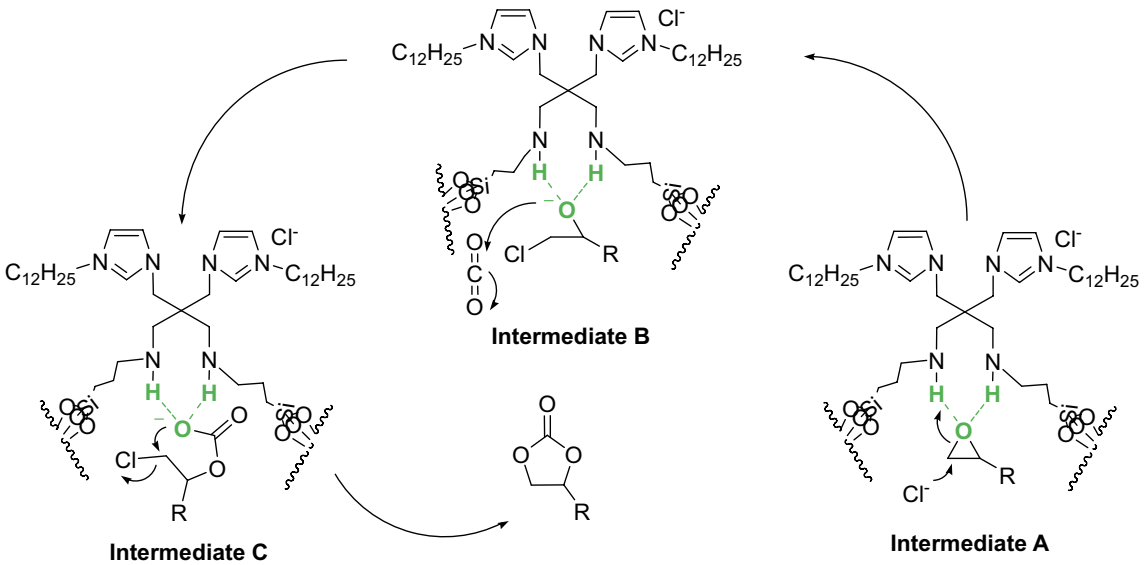

Scheme 3 Proposed catalytic cycle of the fixation of CO_2 by epoxides

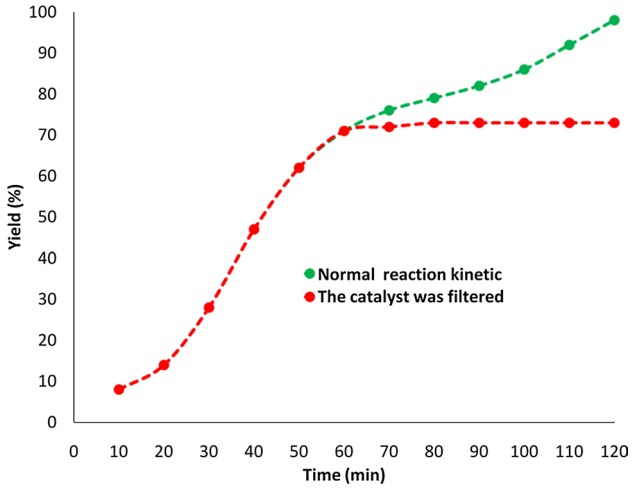

Fig. 9 Leaching test for catalyst fixation of CO_2

and how no addition reagent utilize was identified when the catalyst was removed from the combination (signed as a red curve).

We have explored the scope for scale-up of organic chemistry using a large batch. We performed the reaction on five scales; 1 mol, 1.5 mol, 3 mol, 3.5 mol, and 5 mol, in each case running the reaction. It proved to be very scalable, affording isolated yields of 94%, 96%, 98%, 98%, and 97%, respectively, at the five reaction scales (Fig. 10). This unit should prove an effective tool for the development of scale-up chemistry.

The catalyst reusability of the IL/DFNS nanoparticles was additionally investigated. It was found that it can be reused up to ten times without high loss in its catalytic activity, an outlook necessary perspective of clean chemistry. The catalyst reusability of the IL/DFNS NPs up to successive ten-times, was additionally investigated for catalyst fixation of CO_2 under optimized conditions. It was demonstrated that it can be reused for ten-times without considerable loss in its catalytic activity, a necessary perspective of clean chemistry. It can be rapidly recycled utilizing many washings by ethanol. Then, it is dried at 25 °C and was recycled for many times with approximately unaltered catalytic activity (refer to Fig. 11).

Finally, we have investigated after the passage of the 10th catalytic fixation of carbon dioxide at the specified premium conditions with some assay for ensuring whether the recovered catalyst structure was maintained or not (refer to Fig. 12). As can be seen in Fig. 12a XPS, pattern of the reproduced catalyst demonstrated that the structure of catalyst remained completely intact in recycling. In addition, the loading values of the organic materials in the nanoparticles of IL/DFNS are found after ten reuses using TGA. Figure 12b shows that their values are identical to the fresh nano composites. It should be noted that the nano catalyst has not detected any morphological variations, which is demonstrated using the FE-SEM schemes that obtained from the recovered catalyst as seen in Fig. 12c. As seen in Fig. 12d, the TEM scheme shown that the a generic gray and white layers placed on the direct chain of IL are IL/DFNS after the 10 th run.

4 Conclusions

Generally, under moderate conditions, a series of bifunctional IL/DFNS as phase-transfer catalysts for the fixation of CO_2 with epoxides were demonstrated to provide cyclic carbonates in good to excellent yields. These bifunctional catalysts were easily prepared and structure-tuneable, as well as prove high efficiency for the CO_2 fixation under ambient pressure. In addition, this catalyst are produced for the kinetic resolution of rac-epoxides using CO_2 for producing chiral cyclic carbonates.

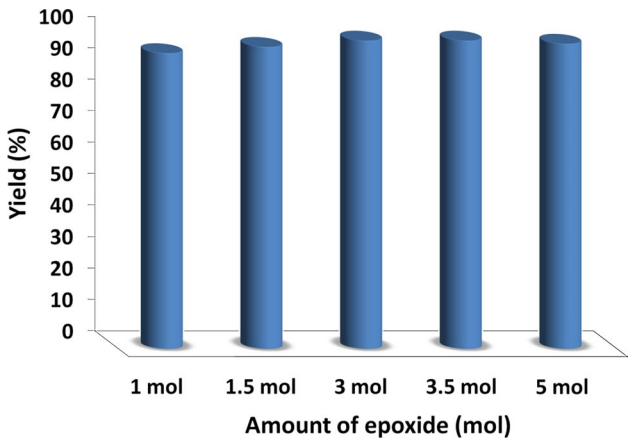

Fig. 10 Reactions performed in the scale-up

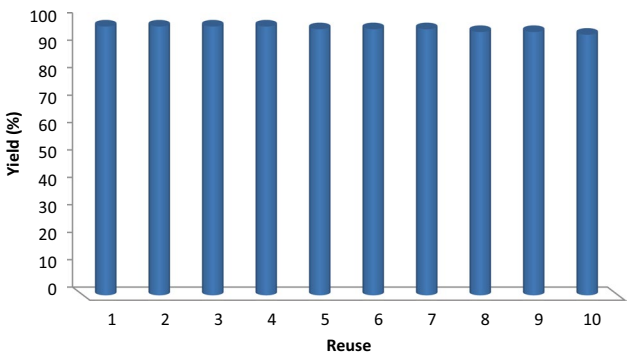

Fig. 11 The reusability of catalysts for catalyst fixation of CO_2

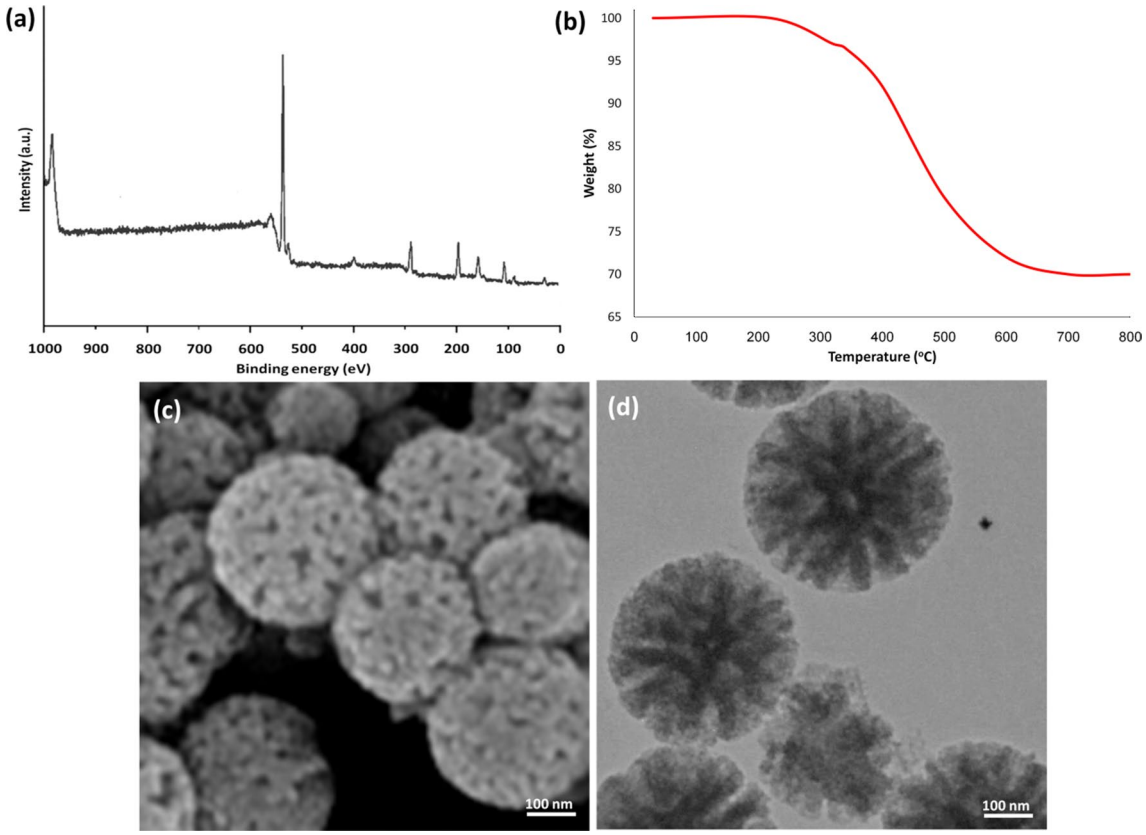

Fig. 12 **a** XPS, **b** TGA, **c** FE-SEM, and **d** TEM images of the recovered IL/DFNS NPs after the 10th run for catalytic fixation of CO_2

References

1. Yuan ZH, Eden MR (2016) Ind Eng Chem Res 55:3383–3419
2. Aresta M, Dibenedetto A, Angelini A (2014) Chem Rev 114:1709–1742
3. Verma S, Baig RBN, Nadagouda MN, Varma RS (2016) Green Chem 18:4855–4858
4. Bhanja P, Modak A, Bhaumik A (2018) Chem Euro J 24:7278–7297
5. Chowdhury AH, Bhanja P, Salam N, Bhaumik A, Islam SM (2018) Mole Catal 450:46–54
6. He H, Perman JA, Zhu G, Ma S (2016) Small 12:6309–6324
7. Kumar A, Madden DG, Lusi M, Chen KJ, Daniels EA, Curtin T, Perry JJ, Zaworotko MJ (2015) Angew Chem Int Ed 54(48):14372–14377
8. Kang XC, Zhu QG, Sun XF, Hu JY, Zhang JL, Liu ZM, Han BX (2016) Chem Sci 7:266–273
9. He ZH, Qian QL, Ma J, Meng QL, Zhou HC, Song JL, Liu ZM, Han BX (2016) Angew Chem Int Ed 55(2):737–741
10. Liang J, Huang YB, Cao R (2019) Coord Chem Rev 378:32–65
11. Lanzafame P, Centi G, Perathoner S (2014) Chem Soc Rev 43:7562–7580
12. Alper E, Orhan OY (2017) Petroleum 3:109–126
13. Ghosh S, Molla RA, Kayal U, Bhaumik A, Islam SM (2019) Dalton Trans 48:4657–4666
14. Markewitz P, Kuckshinrichs W, Leitner W, Linssen J, Zapp P, Bongartz R, Schreiber A, Meller TE (2012) Energy Environ Sci 5:7281–7305
15. Li PZ, Wang XJ, Liu J, Phang HS, Li Y, Zhao Y (2017) Chem Mater 29:9256–9261
16. Patel P, Parmar B, Kureshy RI, Khan NH, Suresh E (2018) ChemCatChem 10:2401–2408
17. Kaneko S, Shirakawa S (2017) ACS Sustain Chem Eng 5:2836–2840
18. Wang L, Zhang G, Kodama K, Hirose T (2016) Green Chem 18:1229–1233
19. Taherimehr M, de Voorde BV, Wee LH, Martens JA, De Vos DE, Pescarmona PP (2017) ChemSusChem 10:1283–1291
20. Arayachukiat S, Kongtes C, Barthel A, Vummaleti SVC, Poater A, Wannakao S, Cavallo L, D'Elia V (2017) ACS Sustain Chem Eng 5:6392–6397
21. Peng J, Wang S, Yang HJ, Ban B, Wei Z, Wang L, Lei B (2018) Fuel 224:481–488
22. Pramudita RA, Motokura K (2018) Green Chem 20:4834–4843
23. Cherubini-Celli A, Mateos J, Bonchio M, Dell'Amico L, Companyó X (2018) ChemSusChem 11:3056–3070
24. Zhang Z, Ye JH, Wu DS, Zhou YQ, Yu DG (2018) Chem Asian J 13:2292–2306
25. Alves M, Grignard B, Mereau R, Jerome C, Tassaing T, Detrembleur C (2017) Catal Sci Technol 7(13):2651–2684
26. Song QW, Zhou ZH, He LN (2017) Green Chem 19:3707–3728
27. Cokoja M, Wilhelm ME, Anthofer MH, Herrmann WA, Kühn FE (2015) ChemSusChem 8:2436–2454
28. Fiorani G, Guo WS, Kleij AW (2015) Green Chem 17:1375–1389
29. Fontaine FG, Courtemanche MA, Légaré MA (2014) Chem Eur J 20:2990–2996

30. Niemi T, Perea-Bucet JE, Fernández I, Hiltunen OM, Salo V, Rautiainen S, Räisänen MT, Repo T (2016) Chem Eur J 22:10355–10359
31. Xin Z, Lescot C, Friis SD, Daasbjerg K, Skrydstrup T (2015) Angew Chem Int Ed 54(23):6862–6866
32. Zhang WZ, Liu S, Lu XB (2015) Beilstein J Org Chem 11:906–912
33. Yang LH, Wang HM (2014) ChemSusChem 7:962–998
34. Liu AH, Dang YL, Zhou H, Zhang JJ, Lu XB (2018) ChemCatChem 10:2686–2692
35. Desens W, Werner T (2016) Adv Synth Catal 358:622–630
36. Wang YB, Sun DS, Zhou H, Zhang WZ, Lu XB (2015) Green Chem 17:4009–4015
37. Xiao YQ, Kong XQ, Xu ZC, Cao CS, Pang GS, Shi YH (2015) RSC Adv 5:5032–5037
38. Zhou H, Wang YM, Zhang WZ, Qu JP, Lu XB (2011) Green Chem 13:644–650
39. Riduan SN, Zhang Y, Ying JY (2009) Angew Chem Int Ed 48(18):3322–3325
40. Rostami A, Mahmoodabadi M, Ebrahimi AH, Khosravi H, Al-Harrasi A (2018) ChemSusChem 11:4262–4268
41. Büttner H, Steinbauer J, Wulf C, Dindaroglu M, Schmalz HG, Werner T (2017) ChemSusChem 10:1076–1079
42. Vara BA, Struble TJ, Wang W, Dobish MC, Johnston JN (2015) J Am Chem Soc 137:7302–7305
43. Hajipour AR, Heydari Y, Kozehgary G (2015) RSC Adv 5:61179–61183
44. Courtemanche MA, Legaré MA, Maron L, Fontaine FG (2013) J Am Chem Soc 135:9326–9329
45. Courtemanche MA, Pulis AP, Rochette E, Légaré MA, Stephan DW, Fontaine FG (2015) Chem Commun 51:9797–9800
46. Ema T, Fukuhara K, Sakai T, Ohbo M, Bai FQ, Hasegawa J (2015) Catal Sci Technol 5(4):2314–2321
47. Whiteoak CJ, Nova A, Maseras F, Kleij AW (2012) ChemSusChem 5:2032–2038
48. Hardman-Baldwin AM, Mattson AE (2014) ChemSusChem 7:3275–3278
49. Zhang JM, Sun J, Zhang XC, Zhao YS, Zhang SJ (2011) Greenhouse Gases. Sci Technol 1:142–159
50. Xu BH, Wang JQ, Sun J, Huang Y, Zhang JP, Zhang XP, Zhang SJ (2015) Green Chem 17:108–122
51. He Q, O'Brien JW, Kitselman KA, Tompkins LE, Curtis GCT, Kerton FM (2014) Catal Sci Technol 4(6):1513–1528
52. Babu R, Kurisingal JF, Chang JS, Park DW (2018) ChemSusChem 11:924–932
53. Zheng DN, Wang TF, Zhu XR, Chen C, Ren TG, Wang L, Zhang JL (2018) Mol Syst Des Eng 3:348
54. Shekari H, Sayadi M, Rezaei M, Allahresani A (2017) Surf Interfaces 8:199–205
55. Maity A, Polshettiwar V (2017) ChemSusChem 10:3866–3913
56. Sadeghzadeh SM (2016) Microporous Mesoporous Mater 234:310–316
57. Patil U, Fihri A, Emwas AH, Polshettiwar V (2012) Chem Sci 3:2224–2229
58. Wasserscheid PJ, Keim W (2000) Angew Chem Int Ed 39:3772–3789
59. Welton T (1999) Chem Rev 99:2071–2084
60. Peng J, Wang S, Yang HJ, Bana B, Wei Z, Wang L, Lei B (2018) Fuel 224:481–488
61. Sadeghzadeh SM (2016) RSC Adv 6:75973–75980
62. Miao J, Wan H, Shao Y, Guan G, Xu B (2011) J Mol Cat A 348:77–82
63. Sun J, Ren J, Zhang S, Cheng W (2009) Tetrahedron Lett 50:423–426
64. Udayakumar S, Raman V, Shim HL, Park DW (2009) Appl Catal A 368:97–104
65. Lan DH, Chen L, Au CT, Yin SF (2015) Carbon 93:22–31
66. Zhang W, Wang Q, Wu H, Wu P, He M (2014) Green Chem 16:4767–4774
67. Xiao L, Su D, Yue C, Wu W (2014) J CO_2 Utiliz 6:1–6
68. Sakai T, Tsutsumi Y, Ema T (2008) Green Chem 10:337–434
69. Mirabaud A, Mulatier JC, Martinez A, Dutasta JP, Dufaud V (2015) ACS Catal 5:6748–6752

Publisher's Note Springer Nature remains neutral with regard to jurisdictional claims in published maps and institutional affiliations.